

Cite this: DOI: 10.1039/

c0xx00000x

ARTICLE TYPE

Ethyleneglycol Tungsten Complexes of calix[6 and 8]arenes: Synthesis, Characterization and ROP of ϵ -caprolactone

Yuanzhuo Li,^a Ke-Qing Zhao,^a Chun Feng,^a Mark R.J. Elsegood,^b Timothy J. Prior,^c Xinsen Sun,^c and Carl Redshaw^{a,c,*}

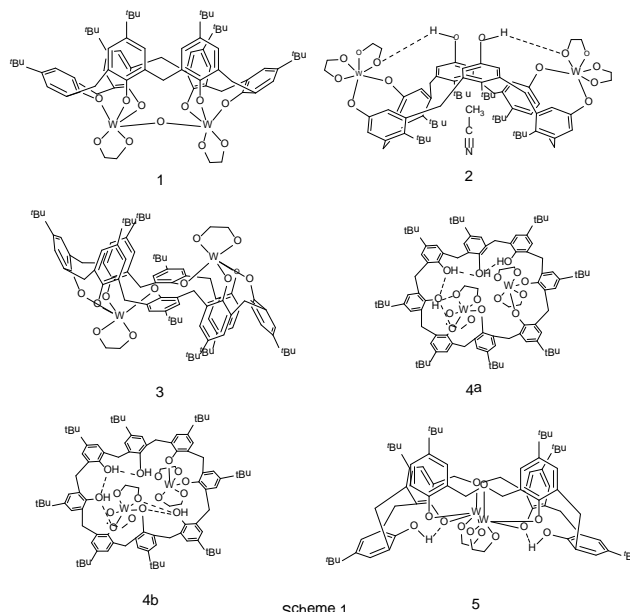
⁵ Received (in XXX, XXX) Xth XXXXXXXXXX 20XX, Accepted Xth XXXXXXXXXX 20XX

DOI: 10.1039/b000000x

ABSTRACT: By varying the reaction conditions, the reaction of [W(eg)₃] (eg = 1,2-ethanediolato) with *p*-*tert*-butylcalix[*n*]areneH_{*n*} (*n* = 6 or 8) in refluxing toluene affords, following work-up, a number of products which have been fully characterized. From the reaction of *p*-*tert*-butylcalix[6]areneH₆ with one or two equivalents of [W(eg)₃], only the oxo-bridged complex {[W(eg)₂(μ-O)*p*-*tert*-butylcalix[6]arene} (1) could be isolated, whereas the use of four equivalents of [W(eg)₃], in the presence of molecular sieves, afforded {[W(eg)₂]₂*p*-*tert*-butylcalix[6]areneH₂}·2MeCN (2); molecules of 2 pack in bi-layers. Under similar conditions, use of one or two equivalents of [W(eg)₃] and *p*-*tert*-butylcalix[8]areneH₈ afforded {[W(eg)₂]₂*p*-*tert*-butylcalix[8]arene}·MeCN (3) in which each tungsten centre was bound by four calixarene oxygens. By contrast, the small orange prisms resulting from the use of four equivalents of [W(eg)₃] and *p*-*tert*-butylcalix[8]areneH₈ were shown by synchrotron radiation to be a mixture of two isomers (4a/4b)·3.5MeCN. In the major isomer {1,2-[W(eg)₂]₂*p*-*tert*-butylcalix[8]areneH₄} (4a), two tungsten centres bind to neighbouring sets of phenolate oxygens, whereas in the minor isomer {1,3-[W(eg)₂]₂*p*-*tert*-butylcalix[8]areneH₄} (4b), there is a protonated phenolic group between the two pairs of phenolate oxygens bound to tungsten; the major:minor ratio is about 83:17. Use of *p*-*tert*-butyltetrahydrodioxacalix[6]areneH₆ with two equivalents of [W(eg)₃] resulted in the isolation of {[WO(eg)₂]₂*p*-*tert*-butyltetrahydrodioxacalix[6]areneH₂} (5)·0.83toluene·MeCN, in which each dimethyleneoxa bridge is bound to an oxotungsten(VI) centre. Complexes 1 – 5, together with the known complex [W(eg)*p*-*tert*-butylcalix[4]arene} (6), have been screened for their ability to ring open polymerize (ROP) ϵ -caprolactone; for 1, 2 and 5, 6 conversion rates were good (> 88 %) at 110 °C over 12 or 24 h, whereas the calix[8]arene complexes 3 and 4 under the same conditions were inactive.

Introduction

The larger calix[*n*]arenes (*n* > 4) continue to be of interest, primarily due to their ability to accommodate multiple metal centres simultaneously.¹ This is desirable since metals in close proximity have the potential to communicate, which in turn may lead to beneficial effects in areas such as magnetism^{2a} or catalysis.^{2b} However, the controlled synthesis of specific polymetallic calix[*n*]arenes can be problematic, often complicated by alkali-metal incorporation or fortuitous hydrolysis and/or oxygenation reactions.³ In the case of tungsten (WCl₆), we have previously shown that by varying the reaction stoichiometry, it is possible to control the degree of metallation.⁴



Scheme 1

5

^a College of Chemistry and Materials Science, Sichuan Normal University, Chengdu, 610066, China.

^b Chemistry Department, Loughborough University, Leicestershire, LE11 3TU, UK

^c Department of Chemistry, University of Hull, Hull, HU6 7RX, UK
E-mail: c.redshaw@hull.ac.uk Fax: +44 1482 466410 Tel: +44 1482 465219.

The only other tungsten calix[*n*]arenes (*n* > 4) that have been reported are the oxo species {[WOC_l]₂p-*tert*-butylcalix[6]areneH₂} and {[WO(NCMe)]₂p-*tert*-butylcalix[8]arene}⁵, the hydrazido complex {[W(NNPh₂)]₂p-*tert*

-butylcalix[6]arene}⁶ plus the p-*tert*-butylcalix[5]arene complexes prepared by Lattmann *et al.*⁷

In terms of the ring opening polymerization (ROP) of ε-caprolactone, few group VI systems appear to have been reported.⁸

Herein, we report a number of new tungstocalix[*n*]arene systems (see scheme 1), resulting from the reaction of [W(eg)₃] (eg = 1,2-ethanediolato) and p-*tert*-butylcalix[6 and 8]areneH_{6,8} or p-*tert*-butyltetrahydrodioxacalix[6]areneH₆. The new tungstocalix[6 and 8]arenes have been fully characterized, and their potential as catalysts for the ROP of ε-caprolactone has been evaluated. We also note that the coordination chemistry of oxacalixarene-type ligands is particularly scant.⁹

Results and Discussion

p-*tert*-butylcalix[6]areneH₆ chemistry

Reaction of p-*tert*-butylcalix[6]areneH₆ with one or two equivalents of [W(eg)₃] in refluxing toluene afforded, after extraction into hot acetonitrile, the orange/red complex {[W(eg)₂(μ-O)p-*tert*-butylcalix[6]arene} (**1**). The isolated yield of **1**, though still only moderate, was greater when two equivalents of [W(eg)₃] were employed, *i.e.* ca. 35 % versus ca. 20 % (for one equivalent). In the IR spectrum of **1**, the band at 966 cm⁻¹ is tentatively assigned to the bridging oxo group; the latter presumably arises via fortuitous hydrolysis. The ¹H NMR spectrum is consistent with the solid-state structure, *vide infra*.

Crystals of **1** suitable for an X-ray structure determination were grown from a hot, saturated solution of acetonitrile on slow cooling and prolonged standing at ambient temperature. The compound crystallizes in the non-centric space group C₂ with the two halves of the compounds related by a two-fold rotation. Two views of the molecular structure are shown in Figure 1, with selected bond lengths and angles given in the caption. Each tungsten centre adopts a distorted octahedral geometry and these are linked via a near linear oxo bridge [W(1) – O – W(1)^{*i*} = 164.7(6)°; W(1) – O(4) = 1.8953(14) Å, symmetry operator *i* = –x, y, –z]. Each tungsten is further bound by three calix[6]arene phenoxide groups and a bi-dentate 1,2-ethanediolato group. The conformation of the calixarene ring is best described as an enlarged cup, for which the *tert*-butyl groups all point up from the bowl.

The analogous reaction using four equivalents of [W(eg)₃] afforded pale yellow crystals of {[W(eg)₂]₂p-*tert*-butylcalix[6]areneH₂}·2MeCN (**2**) in about 45 % isolated yield. Small crystals of **2**·2MeCN suitable for an X-ray structure determination using synchrotron radiation were grown from a hot, saturated solution of acetonitrile on slow cooling and prolonged standing at ambient temperature. The asymmetric unit comprises one molecule of **2** and two molecules of acetonitrile. The molecular structure is shown in Figure 2, with selected bond lengths and angles given in the caption. The geometry about each tungsten is again distorted octahedral, but in this case, each metal is bound by only two of the calixarene phenolate oxygen atoms.

For each metal, one of the 1,2-ethanediolato ligands is involved in H-bonding to one of the remaining calixarene phenolic groups.

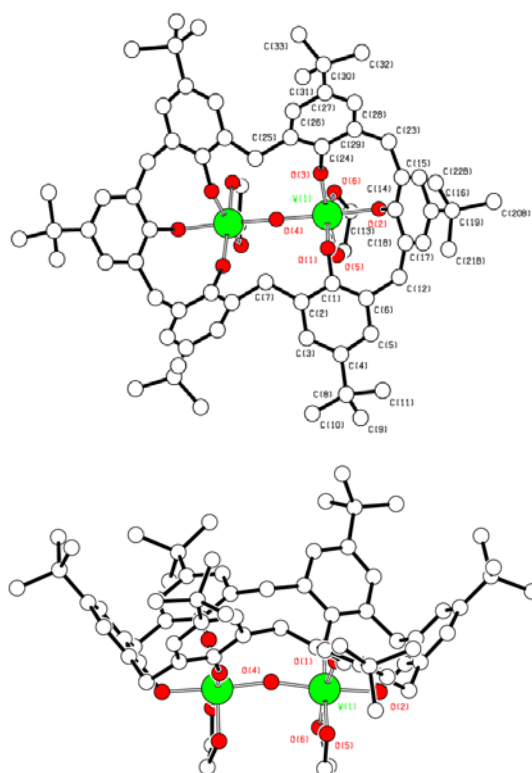


Figure 1 Two views to emphasize the calix[6]arene conformation in **1**. Selected bond lengths (Å) and angles (°): W(1) – O(1) 1.873(7), W(1) – O(2) 1.943(4), W(1) – O(3) 1.877(5), W(1) – O(4) 1.8953(14), W(1) – O(5) 1.899(7), W(1) – O(6) 1.855(6); O(1) – W(1) – O(2) 86.9(3), O(4) – W(1) – O(5) 94.3(3), W(1) – O(1) – W(1)^{*i*} 164.7(6). (Symmetry operator *i* = –x, y, –z)

The conformation of the calix[6]arene ligand is best described as an enlarged cup, with the phenolic rings bearing O(3) and O(6) forming the base. One of the two molecules of acetonitrile is encapsulated within the cup. Molecules of **2** pack in bi-layers with adjacent *tert*-butyl groups at one interface and inter-digited eg groups at the other (see Figure 3).

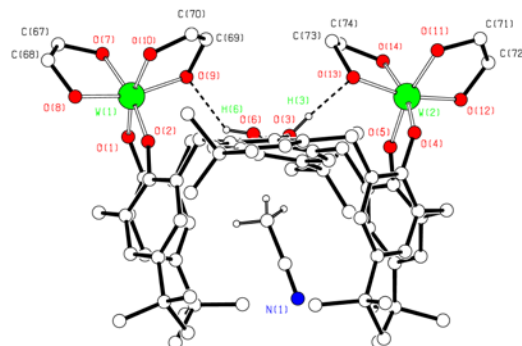


Figure 2. Selected bond lengths (Å) and angles (°) for **2**·2MeCN: W(1) – O(1) 1.847(6), W(1) – O(2) 1.913(6), W(2) – O(4) 1.855(5), W(2) – O(5) 1.922(5); O(1) – W(1) – O(2) 88.0(3), O(7) – W(1) – O(10) 163.5(3), O(4) – W(2) – O(5) 86.5(2), O(11) –

W(2) – O(14) 164.3(2).

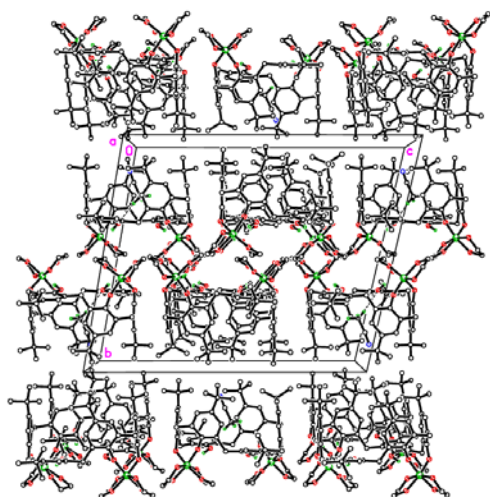


Figure 3. Bi-layer packing of 2·2MeCN.

5 *p*-tert-butylcalix[8]areneH₈ chemistry

On extending the synthetic methodology to *p*-tert-butylcalix[8]areneH₈, use of one or two equivalents of [W(eg)₃] led to the isolation of the red complex [W(eg)₃]2*p*-tert-butylcalix[8]arene} (**3**) in good isolated yield (*ca.* 60 % for two equivalents and *ca.* 40 % for one equivalent).

Large crystals (see ESI, Figure S1) of 3·MeCN suitable for an X-ray structure determination were grown from a hot, saturated solution of acetonitrile on slow cooling and prolonged standing at ambient temperature. The asymmetric unit comprises only one molecule of **3**. The molecular structure is shown in Figure 4, with selected bond lengths and angles given in the caption.

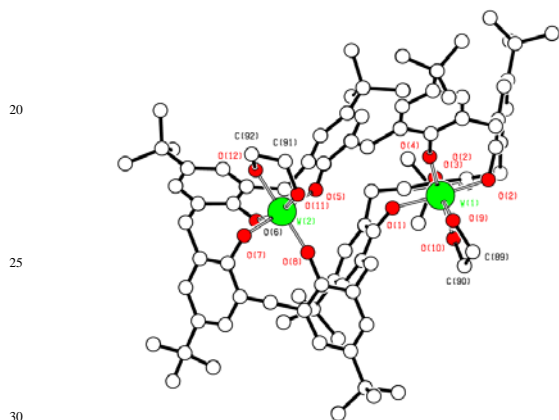


Figure 4. Molecular structure of compound 3·MeCN. Selected bond lengths (Å) and angles (°): W(1) – O(1) 1.908(3), W(1) – O(2) 1.864(3), W(1) – O(3) 1.954(3), W(1) – O(4) 1.861(3), W(2) – O(5) 1.883(2), W(2) – O(6) 1.883(3); W(1) – O(1) – C(1) 1.34.5(2), O(1) – W(1) – O(3) 171.89(11), O(2) – W(1) – O(4) 101.06(12).

The *p*-tert-butylcalix[8]arene is fully deprotonated and adopts a twisted conformation to accommodate, on opposite sides of the molecule, the binding of the two pseudo-octahedral tungsten centres. Each tungsten centre is an average 0.955(7) Å out of the

plane of the calix[8]arene ring. Similar conformations were reported for the complexes {[WO(NCMe)]₂*p*-tert-butylcalix[8]arene}⁵ and {[MCl₂]₂*p*-tert-butylcalix[8]arene} (M = Nb¹⁰ or W⁴).

Increasing the amount of [W(eg)₃] (to four equivalents) resulted in the formation of an orange crystalline solid, however the ¹H NMR spectrum is somewhat different (more complicated) to that of **3**. Interestingly, a crystal structure determination, requiring the use of synchrotron radiation, revealed that the product was a mixture of isomers. In the major isomer (Figure 5, top), the two tungsten centres bind to neighbouring pairs of phenolate oxygens. For this isomer, all phenolic protons (at O(5), O(6), O(7) and O(8)) were located, but not for O(2) in the minor component

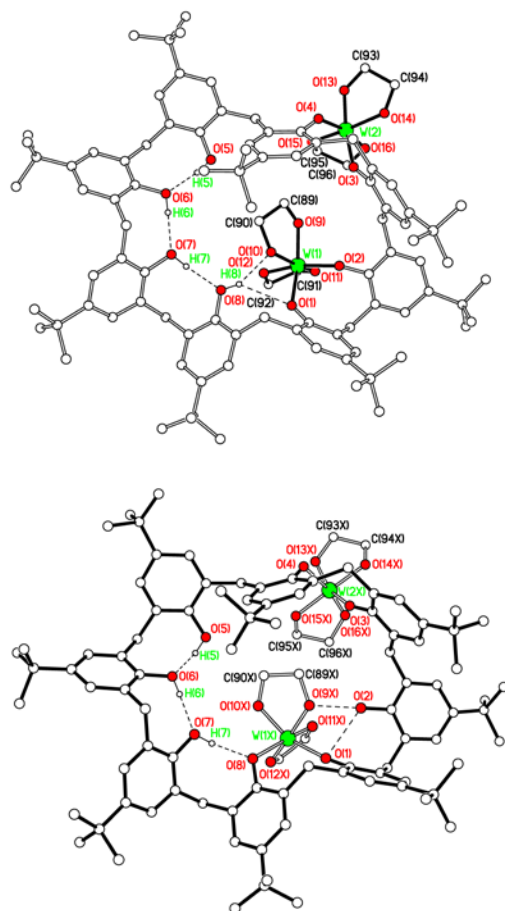


Figure 5. Top, molecular structure of the major isomer **4a**; bottom, molecular structure of minor isomer **4b**. Selected bond lengths (Å) and angles (°): Major: W(1) – O(1) 1.954(4), W(1) – O(2) 1.904(4), W(2) – O(3) 1.912(4), W(2) – O(4) 1.761(6), W(1) – O(9) 1.896(5), W(1) – O(10) 1.942(5); O(1) – W(1) – O(2) 89.58(19), O(1) – W(1) – O(9) 159.5(2), O(3) – W(2) – O(4) 89.3(2). Minor: W(1X) – O(1) 1.855(4), W(2X) – O(3) 1.861(4), W(2X) – O(4) 2.242(7), W(1X) – O(8) 2.150(5), W(1X) – O(9X) 1.88(2), W(1X) – O(10X) 1.88(2); O(1) – W(1X) – O(12X) 104.9(8), O(1) – W(1X) – O(9X) 78.8(6), O(3) – W(2X) – O(4) 77.4(2).

In the minor isomer, this phenolic group O(2) resides between

pairs of bonding phenolate oxygens. The tungsten centres and the eg ligands are disordered such that W(1):W(1X) = 83.39:16.61(8) % and W(2):W(2X) = 62.6:37.4(5) % (same occupancy for the attached eg ligands). The W(1):W(1X) gives the isomer ratio, whereas W(2):W(2X) is more of a conformational issue, probably partially depending on the location of W(1) or W(1X).

The acetonitrile containing N(1) lies in the cleft between phenols containing O(5) and O(6). That containing N(3) lies between O(1) and O(2), whilst those containing N(2) and N(4) lie *exo* to the calixarene, between complexes.

p-tert-butyltetrahomodioxacalix[6]areneH₆ chemistry

Reaction of *p*-tert-butyltetrahomodioxacalix[6]areneH₆ with two equivalents of [W(eg)₃] afforded the yellow complex

{[WO(eg)]₂*p*-tert-

butyltetrahomodioxacalix[6]areneH₂}·0.83toluene·MeCN

(**5**·0.83toluene·MeCN), which exhibited a band in the IR spectrum at 965 cm⁻¹ assigned to νW=O. Single crystals suitable for X-ray diffraction were obtained from a saturated acetonitrile solution at ambient temperature. The compound crystallizes in the centrosymmetric space group *P*2₁/*c* with a single molecule comprising the asymmetric unit. The calixarene binds two W(VI) cations through two adjacent phenoxide groups and a single oxo-bridge in a *fac* arrangement (see Figure 6); for an alternative view, see ESI (Fig. S2). The coordination about each W is completed by oxide (W=O bond lengths are 1.693(5) and 1.702(5) Å) and a bidentate 1,2-ethanediolato ligand. (W–O bond lengths for this ligand are around 1.9 Å. This is consistent with other similar structures in the CSD that contain this ligand.¹¹ The ring is folded such that the two W ions lie at opposite corners of a rectangle. Two of the phenol groups are not deprotonated and form intramolecular hydrogen bonds to phenoxide within the ring.

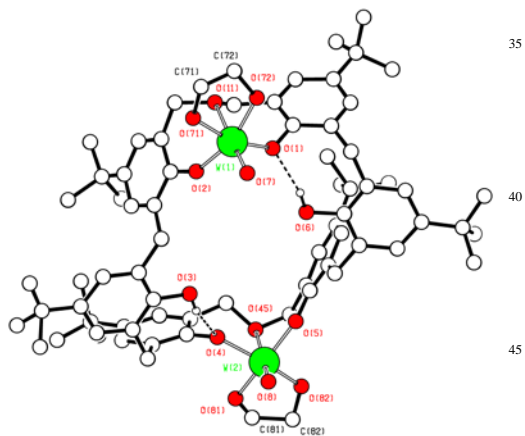


Figure 6. View of the molecular structure of **5**. Selected bond lengths (Å) and angles (°): W(1) – O(1) 1.906(4), W(1) – O(2) 1.891(4), W(1) – O(7) 1.908(4), W(1) – O(11) 2.394(4), W(2) – O(4) 1.941(4), W(2) – O(5) 1.879(4), W(2) – O(8) 1.890(4), W(2) – O(45) 2.403(4); O(7) – W(1) – O(11) 172.46(19), O(8) – W(2) – O(45) 174.21(19).

Ring opening polymerization screening

The complexes **1** – **5** have been screened for their ability to ring open polymerize ε-caprolactone in the presence of benzyl

alcohol (BnOH). For comparison, the known complex [W(eg)*p*-tert-butylcalix[4]arene] (**6**),¹² has also been investigated. Compound **2** was used to optimize the polymerization conditions and the results are tabulated in Table 1.

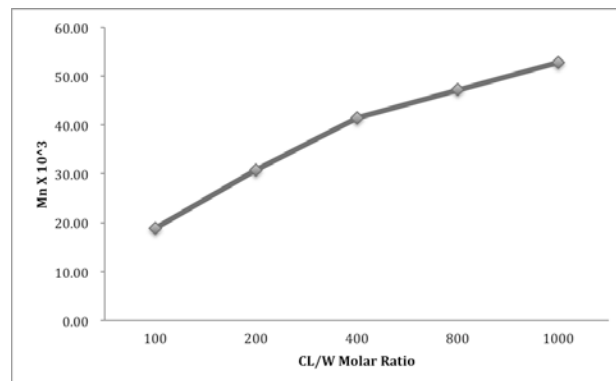


Figure 7. Plots of *M_n* values vs. CL/Al molar ratio in the ROP of ε-CL initiated by **2** (Table 1, entries 3, and 12–16).

It was necessary to activate **2** for the ROP of ε-caprolactone using BnOH. Good conversions were only achieved at temperatures over 100 °C, over prolonged periods (> 12 h), e.g. see runs 1 – 3 versus 4 – 6 (Table 1). Based on entries 1 to 5, there is a near linear relationship between monomer conversion and number average molecular weight (*M_n*), with narrow molecular weight distributions (≤1.34). Moreover, a linear relationship between [CL]/[W] and *M_n* indicates the classical feature of a living process (see Fig. 7). On increasing the temperature beyond 110 °C, the conversion rates and average molecular weight values (*M_n*) decreased, suggesting that 110 °C is more favourable for catalyst stability. Increasing the molar ratio of ε-CL:W from 100:1 to 1000:1 (runs 13 – 16, Table 1) led to an increase in the observed molecular weights 18.82 × 10³ to 52.83 × 10³, which is a desirable scenario given higher molecular weight polyesters possess better mechanical properties. However, although there was little change in the molecular weight distribution (1.36 – 1.83), the conversion rate dropped considerably (from 99 % to 56 %).

Using the optimized conditions for **2**, we also screened the complexes prepared herein as well as the known [W(eg)*p*-tert-butylcalix[4]arene] (**6**).¹² Results in Table 2 revealed good conversions for those systems derived from calix[6]arene ligands (**1** and **2**), although unlike for ethylene polymerization, we did not observe any beneficial effects (versus methylene, –CH₂–) herein when using the dioxamethylene (–CH₂OCH₂–) bridged complex **5**. Surprisingly, the systems **3** and **4** derived from calix[8]arene ligands were inactive under similar conditions. The reason for this is not clear, but may be related to the increased conformational flexibility of the calix[8]arene ligand which somehow hinders the ring opening polymerization process. Furthermore, the known complex [W(eg)*p*-tert-butylcalix[4]arene] (**6**) was found to be active, affording a conversion rate of 74 %, somewhat lower than observed for the calix[6]arene-based systems.

In terms of polymer characterization (molecular weight determination and end group analysis), ¹H and ¹³C NMR spectra of selected polymers (entries 1, 2 and 5, Table 2) were recorded

(see ESI, Figures S3 – S10). Signals at around δ 7.37 and 5.15 ppm ($C_6H_5CH_2-$), and 3.67 ppm (CH_2CH_2OH), with an integrational ratio of 5:2:2, indicated that the polymer chains are capped by a benzyl ester group and a hydroxy end group. This suggests that the polymerization occurs through insertion of a benzyl alkoxy group into CL. The MALDI-TOF spectra (ESI, Figures S11 - S13) revealed the presence of the benzyloxy initiating group and a series of peaks separated by 114.14 mass units.

In summary, a number of new tungstocalix[6 and 8]arenes have been prepared using the metal precursor $[W(eg)_3]$ ($eg = 1,2$ -ethanediolato) and the calix[n]arenes p -*tert*-butylcalix[6 and 8]arene $H_{6,8}$ or p -*tert*-butyltetrahomodioxacalix[6]arene H_6 . Crystal structure determinations reveal a preference for binding two metal centres, though in the solid-state, the relative positions of the metal centres at the lower rim of the calixarene can vary, for example 1,2- $[W(eg)_2]_2$ versus 1,3- $[W(eg)_2]_2$ p -*tert*-butylcalix[8]arene H_4 . The syntheses are sensitive to the presence of air and/or moisture, and the work herein includes the characterization of two oxotungsten species. In terms of the ROP of ϵ -caprolactone, only negligible polymer was isolated at temperatures below 100 °C. At 110 °C, all tungstocalix[6]arenes afforded good conversions (> 80 %) over 12 or 24 h; no benefits were seen for methylene ($-CH_2-$) versus dimethyleneoxa bridges whereas a known tungstocalix[4]arene complex was active, though less so than the calix[6]arene systems. These results suggest that there is a benefit to having two tungsten centres close together when supported by a calix[6]arene, whereas use a calix[8]arene ligand is detrimental to the ROP process, which we tentatively attribute to unfavourable conformational flexibility.

Experimental

General: All manipulations were carried out under an atmosphere of dry nitrogen using conventional Schlenk and cannula techniques or in a conventional nitrogen-filled glove box. Diethyl ether and tetrahydrofuran were refluxed over sodium and benzophenone. Toluene was refluxed over sodium. Dichloromethane and acetonitrile were refluxed over calcium hydride. All solvents were distilled and degassed prior to use. IR spectra (nujol mulls, KBr windows) were recorded on a Nicolet Avatar 360 FT IR spectrometer; 1H NMR spectra were recorded at room temperature on a Varian VXR 400 S spectrometer at 400 MHz or a Gemini 300 NMR spectrometer or a Bruker Advance DPX-300 spectrometer at 300 MHz. The 1H NMR spectra were calibrated against the residual protio impurity of the deuterated solvent. Elemental analyses were performed by the elemental analysis service at the London Metropolitan University and at the University of Hull. Matrix Assisted Laser Desorption/Ionization Time of Flight (MALDI-TOF) mass spectrometry was performed in a Bruker autoflex III smart beam in linear mode, and the spectra were acquired by averaging at least 100 laser shots. 2,5-Dihydroxybenzoic acid was used as the matrix and THF as solvent. Sodium chloride was dissolved in methanol and used as the ionizing agent. Samples were prepared by mixing 20 μ l of matrix solution in THF (2 mg/ml) with 20 μ l of matrix solution (10 mg/ml) and 1 μ l of a solution of ionizing agent (1 mg/ml). Then 1 ml of these mixtures was deposited on a target

plate and allowed to dry in air at ambient temperature. The ligands p -*tert*-butylcalix[6]arene H_6 , p -*tert*-butylcalix[8]arene H_8 and p -*tert*-butyltetrahomodioxacalix[6]arene H_6 were prepared as described in the literature.¹⁰ The precursor $[W(eg)_3]$ and complex **6** were prepared via the methods of Lehtonen and Sillanpää.^{12, 14}

Preparation of $\{[W(eg)_2](\mu-O)p$ -*tert*-butylcalix[6]arene $\}$ (**1**)

Toluene (30 ml) was added to a Schlenk containing p -*tert*-butylcalix[6]arene H_6 (1.40 g, 1.44 mmol) and $[W(eg)_3]$ (1.40 g, 2.91 mmol). After refluxing for 12 h, the volatiles were removed *in-vacuo*, and the residue was extracted into hot (brought to reflux with a heat gun) acetonitrile (30 ml). Prolonged standing (2 - 3 days) at ambient temperature afforded red prisms. Yield 0.75 g, 35.4 %. Elemental analysis calculated for **1**, $C_{70}H_{82}O_{11}W_2$ C 57.1, H 5.6 %; Found C 57.4, H 5.3 %. IR (nujol mull, KBr): 1639 w, 1303 s, 1261 s, 1201 m, 1155 m, 1076 m, 1050 m, 966 m, 936 m, 914 m, 888 m, 857 w, 795 w, 771 m, 723 s, 678 m, 648 w. Mass Spec (EI): 1468 (MH^+). 1H NMR (CD_3CN , 400 MHz) δ : 7.46 (s, 8H, arylH), 7.14 (s, 4H, arylH), 5.90 (s, 8H, OCH_2), 5.05 (d, $^2J_{HH} = 15.2$ Hz, 2H, *endo-CH*₂), 4.81 (d, $^2J_{HH} = 13.2$ Hz, 4H, *endo-CH*₂), 3.51 (d, $^2J_{HH} = 13.2$ Hz, 4H, *exo-CH*₂), 3.39 (d, $^2J_{HH} = 15.2$ Hz, 2H, *exo-CH*₂), 2.17 (s, 12H, 4MeCN), 1.35 (s, 36H, $C(CH_3)_3$), 1.18 (s, 18H, $C(CH_3)_3$).

Preparation of $\{[W(eg)_2]_2p$ -*tert*-butylcalix[6]arene $H_2\} \cdot 2MeCN$ (**2**)

As for **1**, but using p -*tert*-butylcalix[6]arene H_6 (1.40 g, 1.44 mmol) and $[W(eg)_3]$ (1.40 g, 2.91 mmol) and activated molecular sieves. Yield 1.06 g, 44.4 %. Elemental analysis calculated for **2**·MeCN (sample dried *in-vacuo* – MeCN), $C_{77}H_{100.5}N_{1.5}O_{14}W_2$ C 56.4, H 6.2, N 0.9 %; Found C 57.2, H 6.5, N 1.1 %. IR (nujol mull, KBr): 1634 w, 1452 s, 1375 s, 1307 m, 1259 s, 1084 s, 1062s, 1033 s, 963 m, 937 m, 906 m, 884 m, 799 s, 720 m, 643 w, 567 m, 494 w. Mass Spec (EI): 1207 ($M^+ - W - 3egH_2$). 1H NMR ($CDCl_3$, 400 MHz) δ : 7.37 (d, $^4J_{HH} = 2.4$ Hz, 1H, arylH), 7.18 (m, 9H, arylH), 7.03 (overlapping d, 2H, arylH), 5.61 (m, 6H, OCH_2), 5.42 (m, 2H, OCH_2), 5.23 (m, 2H, OCH_2), 5.19 (m, 6H, OCH_2), 3.95 (overlapping d, 4H, *endo-CH*₂), 4.12 (d, $^2J_{HH} = 13.4$ Hz, 2H, *endo-CH*₂), 3.75 (d, $^2J_{HH} = 16.6$ Hz, 2H, *exo-CH*₂), 3.48 (overlapping d, 2H, *exo-CH*₂), 3.32 (d, $^2J_{HH} = 13.2$ Hz, 2H, *exo-CH*₂).

Preparation of $\{[W(eg)]_2p$ -*tert*-butylcalix[8]arene $\}$ (**3**)

As for **1**, but using p -*tert*-butylcalix[8]arene H_8 (0.93 g, 0.72 mmol) and $[W(eg)_3]$ (0.52 g, 1.45 mmol). Yield 0.75 g, 58.7 %. Elemental analysis calculated for **3**·0.5MeCN, $C_{93}H_{113.5}N_{0.5}O_{12}W_2$ C 62.1, H 6.4, N 0.4 %; Found C 61.3, H 6.4, N 0.4 % (sample dried *in-vacuo* for 12 h). IR (nujol mull, KBr): 1596w, 1297m, 1260s, 1208s, 1118s, 1106s, 1071s, 1051s, 936m, 916m, 866s, 829s, 804s, 761m, 723s, 678w, 640s, 616s, 585w, 564w, 535m, 502w, 467w, 430m. Mass Spec (EI): 1818 (M^+), 1800 ($M^+ - 0.5MeCN$), 1788 ($M^+ - MeCN$). 1H NMR (CD_3CN , 600 MHz) δ : 7.48 (d, $^4J_{HH} = 2.4$ Hz, 2H, arylH), 7.29 (d, $^4J_{HH} = 2.4$ Hz, 2H, arylH), 7.24 (d, $^4J_{HH} = 2.4$ Hz, 2H, arylH), 7.17 (d, $^4J_{HH} = 1.8$ Hz, 2H, arylH), 7.13 (d, $^4J_{HH} = 1.8$ Hz, 2H, arylH), 7.00 (d, $^4J_{HH} = 2.4$ Hz, 2H, arylH), 6.97 (d, $^4J_{HH} = 2.4$ Hz, 2H, arylH), 6.29 (d, $^4J_{HH} = 2.4$ Hz, 2H, arylH), 5.78 (m, 2H, OCH_2), 5.58 (m, 2H, OCH_2), 5.45 (m, 2H, OCH_2), 5.13 (m,

2H, OCH₂), 4.68 (overlapping d, 4H, *endo*-CH₂), 4.28 (d, ²J_{HH} = 13.8 Hz, 2H, *endo*-CH₂), 3.65 (d, ²J_{HH} = 16.2 Hz, 2H, *endo*-CH₂), 3.48 (d, ²J_{HH} = 13.2 Hz, 2H, *exo*-CH₂), 3.29 (d, ²J_{HH} = 13.8 Hz, 2H, *exo*-CH₂), 2.80 (d, ²J_{HH} = 12.8 Hz, 2H, *exo*-CH₂), 2.70 (d, ²J_{HH} = 13.2 Hz, 2H, *exo*-CH₂), 2.06 (s, CH₃CN), 1.31 (s, 18H, C(CH₃)₃), 1.21 (s, 18H, C(CH₃)₃), 1.13 (s, 18H, C(CH₃)₃), 0.77 (s, 18H, C(CH₃)₃). * The sample needs to be heated *in vacuo* for 12 h to remove residual egH₂ (δ 3.43 and 2.58 ppm).

Preparation of {1,2-[W(eg)₂]₂p-*tert*-butylcalix[8]areneH₄}/{1,3-[W(eg)₂]₂p-*tert*-butylcalix[8]areneH₄} (4a)/(4b)•3.5MeCN

As for **2**, but using p-*tert*-butylcalix[8]areneH₈ (1.00 g, 0.78 mmol) and [W(eg)₃] (1.11 g, 3.10 mmol). Yield 1.27 g, 79.4 %.

Elemental analysis calculated for **4a/b**•3.5MeCN, C₁₀₃H_{134.5}N_{3.5}O₁₆W₂ C 60.5; H 6.6; N 2.4 %; Found C 60.4, H 6.7, N 2.4 %. IR (nujol mull, KBr): 3183 bw, 1597 w, 1297 m, 1254 s, 1208 s, 1198 s, 1118 m, 1107 m, 1070 m, 1051 m, 945 m, 915 m, 865 m, 830 m, 803 m, 796 m, 760 m, 723 s, 678 w, 641 s, 616 w. Mass Spec (EI): 1922 (MH⁺ – 3MeCN), 1777 (MH⁺ – 3.5MeCN – 2eg), 1715 (MH⁺ – 3.5MeCN – 3eg), 1657 (MH⁺ – 0.5MeCN – W(eg)₂). ¹H NMR (C₆D₆, 500 MHz) δ: 7.36 (m, 2H, arylH), 7.16 (overlapping m, 8H, arylH), 7.00 (overlapping m, 4H, arylH), 6.46 (overlapping d, 2H, arylH), 5.58 (m, 4H, OCH₂), 5.43 (m, 4H, OCH₂), 5.29 (m, 4H, OCH₂), 5.14 (m, 4H, OCH₂),

As for **1**, but using p-*tert*-butyltetrahydrodioxacalix[6]areneH₆ (0.50 g, 0.49 mmol) and [W(eg)₃] (0.36 g, 1.01 mmol). Yield 0.56 g, 69.1 %. Elemental analysis calculated for **5**, C₇₂H₉₂O₁₄W₂ (sample dried *in vacuo* for 12 h): C 55.9, H, 6.0 %; Found C 55.6, H 6.1 %. IR (nujol mull, KBr): 3170 bw, 1635 w, 1304 s, 1155 m, 1077 m, 965 m, 892 m, 846 w, 770 m, 723 s. Mass Spec (EI): 1269 (M⁺ – W(O)(eg)). ¹H NMR (C₆D₆, 500 MHz) δ: 7.52 (m, 2H, arylH), 7.28 (m, 2H, arylH), 7.22 (m, 2H, arylH), 7.16 (m, 2H, arylH), 7.00 (m, 2H, arylH), 6.86 (m, 2H, arylH), 5.63 (m, 4H, OCH₂), 5.20 (m, 4H, OCH₂), 4.97 (m, 2H, OCH₂), 4.88 (m, 4H, OCH₂), 4.78 (m, 2H, OCH₂), 3.96 (overlapping d, 4H, *endo*-CH₂), 3.74 (overlapping d, 4H, *exo*-CH₂), 2.06 (s, CH₃CN), 1.24 (m, 54H, C(CH₃)₃).

Procedure for ROP of ε-caprolactone

Typical polymerization procedures in the presence of one equivalent of benzyl alcohol (Table 2, run 1) are as follows. A toluene solution of **3** (0.010 mmol, 1.0 mL toluene) and BnOH (0.010 mmol) were added into a Schlenk tube in the glove-box at room temperature. The solution was stirred for 2 min, and then ε-caprolactone (2.5 mmol) along with 1.5 mL toluene was added to the solution. The reaction mixture was then placed into an oil bath pre-heated at 110 °C, and the solution was stirred for the prescribed time (24 h). The polymerization mixture was then

Table 1. Ring Opening Polymerization of ε-CL by pre-catalyst **2**.

Entry	Cat.	CL:Al:BuOH	T/°C	t/h	mg	yield (%)	M _n *10 ⁻³	PDI
1	2	400:01:01	170	24	2.74	95.1	30.74	1.33
2	2	400:01:01	140	24	2.79	96.9	36.50	1.33
3	2	400:01:01	110	24	2.82	98.0	41.40	1.34
4	2	400:01:01	80	24	0.32	11.1	1.83	1.28
5	2	400:01:01	50	24	0.21	7.3	1.56	1.24
6	2	400:01:01	20	24	0.08	2.8	1.24	1.23
7	2	400:01:01	110	48	2.8	99.3	40.83	1.58
8	2	400:01:01	110	12	2.72	94.4	9.63	1.44
9	2	400:01:01	110	6	1.13	39.2	3.83	1.27
10	2	400:01:01	110	3	0.56	19.4	3.15	1.28
11	2	400:01:01	110	1	0.11	3.8	1.83	1.25
12	2	400:01:01	110	0.5	0	-	-	-
13	2	100:01:01	110	24	2.85	99.0	18.82	1.36
14	2	200:01:01	110	24	2.84	98.6	30.79	1.42
15	2	800:01:01	110	24	1.84	63.9	47.19	1.52
16	2	1000:01:01	110	24	1.62	56.3	52.83	1.83

^aConditions: 20 μmol of cat.; 1.0 M ε-CL toluene solution. ^bX=W complex ^cGPC data in THF vs polystyrene standards.

4.91 (m, 2H, *endo*-CH₂), 4.47 (overlapping d, 4H, *endo*-CH₂), 4.10 (m, 2H, *endo*-CH₂), 3.46 (overlapping d, 4H, *exo*-CH₂), 3.29 (m, 2H, *exo*-CH₂), 2.91 (m, 2H, *exo*-CH₂), 2.17 (s, 10.5H, MeCN), 1.32 (s, 36H, C(CH₃)₃), 1.31 (s, 18H, C(CH₃)₃), 1.22 (s, 18H, C(CH₃)₃).

quenched by addition of an excess of glacial acetic acid (0.2 mL) into the solution, and the resultant solution was then poured into methanol (200 mL). The resultant polymer was then collected on filter paper and was dried *in vacuo*.

Preparation of {[WO(eg)]₂p-*tert*-butyltetrahydrodioxacalix[6]areneH₂} (5)

Table 2. Ring Opening Polymerization of ϵ -CL by pre-catalysts **1 - 6**.

Entry	Cat.	CL:X ^b :BnOH	T/ ^o C	t/h	m/g	Yield (%)	M _n *10 ^{-3c}	PDI
1	1	400:01:01	110	24	2.53	87.8	28.1	1.23
2	2	400:01:01	110	24	2.82	97.9	41.4	1.34
3	3	400:01:01	110	24	0	-	-	-
4	4	400:01:01	110	24	0	-	-	-
5	5	400:01:01	110	24	2.71	94.1	18.7	1.14
6	6	400:01:01	140	24	2.13	74.0	19.3	1.18
7	6	400:01:01	110	24	2.33	80.9	23.2	1.22
8	6	400:01:01	80	24	1.84	63.9	10.7	1.18

^aConditions: 20 μ mol of cat.; 1.0 M ϵ -CL toluene solution. ^bX=W complex ^cGPC data in THF vs polystyrene standards.

Crystallography

For **1**, **3**, and **5**: Data were collected using an Agilent Xcalibur diffractometer with an Eos CCD detector operating with Mo K α radiation using a series of ω -scans.¹⁵ Data were treated using an empirical absorption correction. For **1** and **5** data collection was conducted at room temperature (293 K). For **3** data were collected with the crystal cooled to 135 K. Structure solution and refinement was conducted using the SHELX suite of programs.¹⁶

Structure of **1**: Two of the three symmetry independent *tert*-butyl groups (C9-C11 and C20-C22) were modelled as disordered over two sets of positions. There was no evidence for inclusion of solvent within the structure. Structure of **3**: No disorder was modelled for the *tert*-butyl groups although these exhibit relatively large displacement parameters, but the core of the calix[8]arene is well determined. Small portions of the structure contained disordered solvent molecules which could not be resolved as point atoms. The Platon SQUEEZE routine¹⁷ was employed to deal with scattering from these regions. For **1** and **3** the unit cell contained four disordered MeCN molecules. Structure of **5**: The central core of the oxacalixarene is well determined but the *tert*-butyl groups show rather larger displacement parameters. The structure contains a single molecule of MeCN within each oxacalixarene bowl and a molecule of toluene (~83 % occupied) that is located on the bottom edge of the oxacalixarene and may be localised by C–H $\cdots\pi$ interactions.

For **2**: Data collected on a Bruker APEX 2 CCD diffractometer at Daresbury SRS station 9.8.¹⁸ The *tert*-butyl groups at C(18) and C(40) were modelled as disordered over two sets of positions. The MeCN in the calixarene cavity was well defined and was modelled as point atoms. Platon SQUEEZE¹⁷ was used to model eight other MeCN molecules per unit cell (one per complex molecule) as diffuse electron density. The structure could also be modelled in the triclinic crystal system, but this led to two very large residual electron density peaks of > 8 eÅ³, so the simpler C2/c solution was deemed more satisfactory. For **4**: Data collected on a Bruker APEX 2 CCD diffractometer at Daresbury SRS station 9.8.¹⁷ Both W(1) and W(2) atoms were modelled as two-fold disordered along with the attached eg groups, with occupancy factors of 83.39:16.61(8)% for the former, and 62.6:37.4(5)% for the latter. The *tert*-butyl group at C(18) was

modelled with all atoms disordered over two sets of positions, while those at C(40) and C(51) were modelled with just the methyl groups split over two sets of positions. One MeCN was 50/50 disordered over a centre of symmetry.

Crystal structure data have been deposited with the CCDC (numbers 989342-989344, 989597, and 1010285). These data can be obtained from of charge from www.ccdc.cam.ac.uk.

Acknowledgments

We thank Sichuan Normal University for financial support. The CCLRC is thanked for the award of beamtime at SRS Daresbury Laboratory (Station 9.8), and the EPSRC Mass Spectrometry Service at Swansea is thanked for data.

References

- For pre-**2003** references, see C. Redshaw *Coord. Chem. Rev.* **2003**, *244*, 45. For post-**2003**, Y. Li, K.-Q. Zhao, C. Redshaw, A. Y. Nuñez, B. A. M. Ortega, S. Memon and T. A. Hanna in *The Chemistry of Metal Phenolates Parts 1 and 2*, Ed. J. Zabicky, Wiley 2014, ISBN: 978-0470973585.
- (a) R. McLellan, S.M. Taylor, R.D. McIntosh, E.K. Brechin and S.J. Dalgarno, *Dalton Trans.*, **2013**, *42*, 6697. (b) D.H. Homden and C. Redshaw, *Chem. Rev.* **2008**, *108*, 5086.
- (a) C. Redshaw, D.H. Homden, D.L. Hughes, J.A. Wright and M.R.J. Elsegood, *Dalton Trans.* **2009**, 1231. (b) A. Arbaoui, C. Redshaw, M.R.J. Elsegood, V.E. Wright, A. Yoshizawa and T. Yamato, *Chem. Asian J.* **2010**, *5*, 621.
- V.C. Gibson, C. Redshaw and M.R.J. Elsegood, *Chem. Comm.* **2002**, 1200.
- C. Redshaw and M.R.J. Elsegood, *Eur. J. Inorg. Chem.* **2003**, 2071.
- C. Redshaw and M.R.J. Elsegood, *Inorg. Chem.* **2001**, *39*, 5164.
- M. Fan, H. Zhang and M. Lattman, *Chem. Commun.* **1998**, 99.
- (a) M. Labet and W. Thielemans, *Chem. Soc. Rev.* **2009**, *38*, 3484. (b) A. Arbaoui and C. Redshaw, *Polym. Chem.* **2010**, *1*, 801. (c) X. Rong and C. Chunxia, *Progress in Chemistry*, **2012**, *24*, 1519.
- (a) S.M. Taylor, R.D. McIntosh, J. Rezá, S.J. Dalgarno and E.K. Brechin, *Chem. Commun.* **2012**, *48*, 9263. (b) R.E. Fairbairn, R. McLellan, R.D. McIntosh, M.A. Palacios, E.K. Brechin and S.J. Dalgarno *Dalton Trans.* **2014**, *43*, 5292.
- C. Redshaw, M. Rowan, D.M. Homden, M.R.J. Elsegood, T. Yamato and C. Péres-Casas, *Chem. Eur. J.* **2007**, *13*, 10129.
- F.H. Allen, *Acta Cryst. B*, **2002**, *58*, 380, see www.ccdc.ac.uk
- A. Lehtonen and R. Sillanpää, *Polyhedron* **1998**, *17*, 3327.
- (a) A. Arduini and A. Casnati in *Macrocyclic Synthesis*, Ed. D. Parker, Oxford University Press, **1996**, chapter 7. (b) B. Masci, *J. Org. Chem.* **2001**, *66*, 1497. (c) B. Dhawan and C.D. Gutsche, *J. Org. Chem.* **1983**, *48*, 1536.
- A. Lehtonen and R. Sillanpää, *Polyhedron* **1994**, *13*, 2519.

-
- 15 CrysAlisPro software for CCD diffractometers, Agilent Technologies, 2012.
 - 16 G.M. Sheldrick, *Acta Crystallogr.* **2008**, *A64*, 112-122.
 - 17 A.L. Spek, *Acta Crystallogr.* **1990**, *A46*, C34.
 - 5 18 SAINT (2006), and APEX 2 (2006) software for CCD diffractometers. Bruker AXS Inc., Madison, USA.

Cite this: DOI: 10.1039/

c0xx00000x

ARTICLE TYPE

Table 3. Crystallographic data for structures **1 - 5**

Formula	C ₇₀ H ₈₂ O ₁₁ W ₂	C ₇₄ H ₉₆ O ₁₄ W ₂ ·2MeCN	C ₉₂ H ₁₁₂ O ₁₂ W ₂	C ₉₆ H ₁₂₄ O ₁₆ W ₂ · 3.5 MeCN	C ₇₂ H ₉₂ O ₁₄ W ₂ · 0.83PhMe·MeCN
Compound	1	2	3	4a/b	5
Formula weight (g mol ⁻¹)	1471.09	1659.31	1777.52	2045.34	1663.05
Crystal system	Monoclinic	Monoclinic	Monoclinic	Triclinic	Monoclinic
Space group	<i>C2</i>	<i>C2/c</i>	<i>P2₁/c</i>	<i>P1</i>	<i>P2₁/c</i>
Temperature (K)	293	150	135	150	293
Unit cell dimensions					
<i>a</i> (Å)	23.4741(8)	42.531(6)	12.2109(2)	14.8901(11)	19.7129(9)
<i>b</i> (Å)	12.0721(4)	14.431(2)	34.2259(5)	17.5516(13)	13.6419(7)
<i>c</i> (Å)	16.8073(5)	25.556(4)	20.5984(3)	22.0164(16)	31.4289(16)
α (°)	90	90	90	112.02119(9)	90
β (°)	116.734(4)	101.4406(17)	92.226(1)	105.3910(10)	104.805(5)
γ (°)	90	90	90	93.0486(10)	90
<i>V</i> (Å ³)	4253.7(2)	15374(4)	8602.2(2)	5067.2(6)	8171.3(7)
<i>Z</i>	2	8	4	2	4
Calculated density (Mg m ⁻³)	1.149	1.434	1.373	1.341	1.352
Absorption coefficient (mm ⁻¹)	2.747	2.671	2.730	2.331	2.871
Transmission factors (max., min)	0.610, 0.503	0.924, 0.617	0.772, 0.611	0.933, 0.679	0.598, 0.480
Crystal size (mm ³)	0.29 × 0.24 × 0.22	0.20 × 0.09 × 0.03	0.20 × 0.15 × 0.10	0.18 × 0.08 × 0.03	0.30 × 0.20 × 0.20
θ_{\max} (°)	26.37	30.97	26.37	30.00	28.56
Reflections measured	6695	95194	17552	60220	18607
Unique reflections, <i>R</i> _{int}	6695, 0.0258	27094 0.1768	17552 0.0536	31223 0.0443	18607 0.0453
Reflections with <i>F</i> ² > 2σ(<i>F</i> ²)	5824	22156	14374	20519	12892
Number of parameters	362	899	979	1435	814
<i>R</i> ₁ , <i>wR</i> ₂ [<i>F</i> ² > 2σ(<i>F</i> ²)]	0.0364, 0.0841	0.0889, 0.1962	0.0387, 0.0738	0.0763, 0.1588	0.0552, 0.1246
GOOF	1.02	1.22	1.07	1.11	1.05
Largest difference peak and hole (e Å ⁻³)	1.296 and -0.645	2.734 and -2.488	1.329 and -0.872	1.318 and -2.295	1.034 and -0.884